Copy 6
RM L51H08

NACA RM L51H08

NACA

RESEARCH MEMORANDUM

A WIND-TUNNEL INVESTIGATION OF THE STATIC STABILITY CHARACTERISTICS OF A $\frac{1}{8}$-SCALE EJECTABLE PILOT-SEAT COMBINATION AT A MACH NUMBER OF 0.8

By Fioravante Visconti and Robert J. Nuber

Langley Aeronautical Laboratory
Langley Field, Va.

NATIONAL ADVISORY COMMITTEE FOR AERONAUTICS

WASHINGTON

December 7, 1951

NACA RM L51H08

NATIONAL ADVISORY COMMITTEE FOR AERONAUTICS

RESEARCH MEMORANDUM

A WIND-TUNNEL INVESTIGATION OF THE STATIC STABILITY CHARACTERISTICS OF A $\frac{1}{8}$-SCALE EJECTABLE PILOT-SEAT COMBINATION AT A MACH NUMBER OF 0.8

By Fioravante Visconti and Robert J. Nuber

SUMMARY

An investigation was made of a $\frac{1}{8}$-scale model of an ejectable pilot-seat combination with and without stabilizing fins. The purpose of this investigation was to determine the static aerodynamic characteristics and the effectiveness of various stabilizing fins at a high subsonic Mach number (0.8).

The results of these tests indicated that the instability of the pilot-seat combination was eliminated by the addition of stabilizing fins. Large changes in the stability characteristics and trim angles resulted from variations in fin position, dihedral, or incidence angles and from small displacements of the center-of-gravity position. The magnitude of the aerodynamic interference that exists about the seat had a large effect on the effectiveness of fins located at moderate distances from the seat.

INTRODUCTION

In efforts to assist designers in providing for a satisfactory type of emergency pilot escape from high-speed aircraft, many flight and wind-tunnel tests have been made of various proposed devices. Flight tests (references 1 and 2) have proved the value of the pilot-ejection seat for emergency pilot escape at least up to moderate subsonic speeds where the use of stabilizing parachute equipment is feasible. At higher speeds, however, the problem of safe pilot departure becomes more acute. A large deceleration caused by the release of a parachute at high speeds is likely to cause injury to the pilot and damage to the parachute. If, on the other hand, the pilot-seat combination is permitted to fall freely

until it has gradually decelerated to a safe parachute-release speed, high rotational velocities that are likely to occur with a body of this nature could very well prove injurious to the pilot.

One method of preventing the high rotational velocities of the seat until it has decelerated sufficiently to allow safe release of a parachute is the use of stabilizing fins. The stabilizing effects of fins on a pilot-ejection seat has been investigated at low and moderate speeds (references 3 and 4). The available literature on the characteristics of fin-stabilized pilot-ejection seats, however, is insufficient to allow accurate prediction of the stability characteristics at high subsonic speeds. Consequently, an investigation of a $\frac{1}{8}$- scale model of an ejectable pilot-seat combination with and without stabilizing fins has been made in the Langley low-turbulence pressure tunnel. At a Mach number of 0.8, the static aerodynamic characteristics and the stabilizing effectiveness of various fins were obtained. Normal forces and chord forces on the seat without fins were also obtained through a Mach number range between 0.4 and 0.88. The tests were made at seat attitudes ranging from -25° to 25° in angle of attack and -4° to 8.8° in angle of yaw. Calculations were also made to show the effects of center-of-gravity displacement on the stability characteristics.

SYMBOLS AND COEFFICIENTS

The direction of the forces and moments are presented in figure 1. The coefficients and symbols used herein are defined as follows:

α	angle of attack, degrees
α_t	trim angle of attack, degrees
ψ	angle of yaw, degrees
C_N	normal-force coefficient $\left(\frac{\text{Normal force}}{q_o S}\right)$
C_C	chord-force coefficient $\left(\frac{\text{Chord force}}{q_o S}\right)$
C_Y	side-force coefficient $\left(\frac{\text{Side force}}{q_o S}\right)$

[redacted]

C_m	pitching-moment coefficient $\left(\frac{\text{Pitching moment}}{q_o Sc}\right)$
C_n	yawing-moment coefficient $\left(\frac{\text{Yawing moment}}{q_o Sc}\right)$
C_l	rolling-moment coefficient $\left(\frac{\text{Rolling moment}}{q_o Sc}\right)$
z/c	vertical displacement of center of gravity
x/c	longitudinal displacement of center of gravity
z	vertical distance, positive upward, inches
x	longitudinal distance, positive forward, inches
c	seat reference length, 6 inches
b	seat span, 2.25 inches
S	seat reference area, 13.5 square inches
q_o	free-stream dynamic pressure
M	free-stream Mach number
ΔH	total-pressure loss ($H_o - H_w$)
H_o	free-stream total pressure
H_w	total pressure in wake
X'	longitudinal location of center of fin, inches
Y'	lateral location of center of fin, inches
Z'	vertical location of center of fin, inches
a_f	length of fin, inches
b_f	width of fin, inches
i_f	angle of incidence of fin, degrees
Γ	dihedral angle of fin, degrees

[redacted]

$$C_{m_\alpha} = \left(\frac{\partial C_m}{\partial \alpha}\right)_\psi$$

$$C_{N_\alpha} = \left(\frac{\partial C_N}{\partial \alpha}\right)_\psi$$

$$C_{C_\alpha} = \left(\frac{\partial C_C}{\partial \alpha}\right)_\psi$$

$$C_{n_\psi} = \left(\frac{\partial C_n}{\partial \psi}\right)_\alpha$$

$$C_{Y_\psi} = \left(\frac{\partial C_Y}{\partial \psi}\right)_\alpha$$

The subscripts to the partial derivatives denote the variable held constant when the partial derivatives were taken.

MODELS AND TESTS

The model tested represented a practical design of an ejectable pilot-seat combination for use on a transonic aircraft. Photographs of the model are presented as figure 2. In order to obtain a high choking Mach number, the model was limited to $\frac{1}{8}$-scale. The seat pan and back were made of steel plate and the frame work was fabricated from $\frac{1}{8}$-inch welding rods. All stabilizing fins were made of $\frac{1}{16}$-inch sheet steel and were attached to the seat by means of $\frac{3}{16}$-inch diameter rods. The dummy pilot was carved from a mahogany block to the dimensions of the average pilot.

Tests were made with and without stabilizing fins. The initial configuration investigated consisted of the ejectable pilot-seat combination without fins and is referred to herein as model configuration 1. Configuration 2 consisted of the seat with stabilizing fins 1.38 inches long and 1.06 inches wide. For configurations 3 to 7, larger fins having lengths and widths of 1.94 and 1.38 inches, respectively, were attached to the seat. The locations of the fin centers with respect to the seat body axes, and the angles of incidence and dihedral are shown in figure 1.

The tests were made in the 3- by $7\frac{1}{2}$- foot rectangular test section of the Langley low-turbulence pressure tunnel (described in references 5 and 6) in an atmosphere of Freon-12. A six-component strain-gage sting balance, on which the model was mounted, was used to measure the normal, chord, and side forces and the pitching, yawing, and rolling moments of configuration 1 and 2. No chord forces were measured for configurations 3 to 7 because of an electrical failure in the internal balance. At a Mach number of 0.8, the forces and moments were obtained for model angles of attack ranging between -25° and 25° at 0° yaw angle and through a yaw-angle range between -4° and 8.88° at angles of attack of -25°, 0°, and 25°. Normal forces and chord forces were also measured for configuration 1 through a Mach number range between 0.4 and 0.88 for angles of attack ranging between -25° and 25° at 0° yaw angle.

CORRECTIONS AND ACCURACY OF DATA

Since the balance system was contained in the model, the aerodynamic forces exerted on the model supports were not measured by the balance. The interference effect of the sting support on the model was not determined. It is believed to be negligible, however, because of the small relative size of the sting and the fact that it was located in a region of separated flow behind the model. The coefficients and Mach numbers were not corrected for tunnel-wall effects; approximate calculations, however, indicated that the maximum corrections to the dynamic pressure and the Mach number existed at a Mach number of 0.88 and did not exceed $0.01q_o$ and 0.01M. The values of the coefficients and Mach numbers as obtained in an atmosphere of Freon-12 were converted to corresponding values in air by the methods presented in reference 6.

An analysis of the accuracy of the strain-gage measurements and the ability to duplicate test points indicated the following maximum variations:

C_N, C_C, C_Y	±0.02
C_m, C_n	±0.002
C_l	±0.003
M	±0.015

The angles of attack and angles of yaw of the model were set within 0.1°.

RESULTS AND DISCUSSION

Stability Characteristics

The results of the tests of the ejectable pilot-seat combination with and without stabilizing fins are presented in figures 3 to 5.

[redacted]

The discussion refers to the data obtained at a Mach number of 0.8 unless otherwise stated.

Fin effectiveness.- The results of tests of the pilot-ejection seat without fins (configuration 1) indicate that although the model was stable in pitch, it would not trim within the angle-of-attack range investigated (fig. 3) and furthermore was unstable in yaw (fig. 4). The addition of small fins (configuration 2) did not trim the model within the angle-of-attack range investigated and actually had a destabilizing effect in pitch.

In order to determine the cause of the adverse effectiveness of the small fins, total-pressure measurements were obtained at the location of the right-hand small fin with the fins removed. These measurements were made at a Mach number of 0.4 with the seat incidence and yaw angles set at 0°. The results, presented in figure 5, indicate that a portion of the fins of configuration 2 were located in the seat wake. It would be expected, however, that since the average dynamic pressure in the region of the fins was found to be as much as 80 percent of the free-stream dynamic pressure (fig. 5), the addition of the fins would give the seat greater stability. Inasmuch as the fins caused the model to become unstable, the adverse fin effectiveness is attributed to large flow angularities which probably exist about a blunt body of this nature.

In order to decrease the effect of the flow angularity on the fins, they were relocated outboard and the dihedral angles were reversed from 45° to -60°. The fins were also increased in size. These changes (configuration 3) resulted in an arrangement which was stable in pitch (fig. 3) and in yaw (fig. 4) but still did not trim within the angle-of-attack range investigated.

Although configuration 3 provides stable pitching- and yawing-moment slopes, it was felt that the longer fin supporting arms may result in unnecessary structural complications. To determine a good compromise between satisfactory fin characteristics and a shorter length of the fin supporting arms, the fins were relocated to positions shown as configurations 4 and 5 in figure 1. The fins of configuration 5 were apparently located too close to the seat (in the region of aerodynamic interference that existed at positive angles of attack) as attested by the data presented in figure 3. Configuration 4 showed stable pitching-moment and yawing-moment characteristics throughout the angle-of-attack range investigated, although in this angle range it did not trim. The supporting arm length and position outboard from the seat center line was considered a good compromise.

In order to decrease the pitch angle of trim, the fin dihedral and incidence angle of configuration 4 were changed from -60° to -45° and -41° to -9°, respectively. Although this fin configuration, referred to

herein as configuration 6, resulted in a model that was stable in pitch and trimmed at an angle of attack of approximately 21°, it was unstable in yaw near the pitch trim angle (figs. 3 and 4(b)). By changing the fin dihedral and incidence angles from -45° to -55° and -9° to 13°, respectively, (configuration 7) the model remained stable in pitch over the angle-of-attack range investigated and neutral stability in yaw at a pitch trim angle of 18.5° was obtained. (See figs. 3 and 4(c)).

Effect of center-of-gravity displacement.- Calculations were made to determine the magnitude of center-of-gravity displacement allowable for favorable stability characteristics on configuration 7, the results of which are presented in figure 6.

The positions of center of gravity that would result in rates of change of pitching-moment coefficient with angle of attack $C_{m_{\alpha_1}}$ equal to 0, -0.001, -0.002, and -0.003 are denoted by the solid curves of figure 6(a). These curves were calculated with the use of the following equation:

$$C_{m_{\alpha_1}} = C_{m_\alpha} - \frac{x}{c} C_{N_\alpha} - \frac{z}{c} C_{C_\alpha} \qquad (1)$$

The values of C_{m_α}, C_{N_α}, and C_{C_α} substituted in this equation represent average slopes measured between angles of attack of 10° and 20°. The limitations imposed on the use of these curves as a result of this assumption is discussed in a subsequent section. It has been noted previously that the chord forces for configuration 7 (large fins) were not measured. Inasmuch as the increment of chord force due to the addition of small fins was found to be a maximum of only 1.1 percent of the total chord force without fins (fig. 3) the additional increment due to the large fins is believed to be negligible. The values of C_{C_α} used in the computations, therefore, were those determined for configuration 2 (small fins).

The loci of center-of-gravity positions for given pitch angles of trim are presented as dashed curves in figure 6(a). The center-of-gravity positions at which the seat would trim in pitch were calculated with the use of the following equation:

$$C_m - \frac{x}{c} C_N - \frac{z}{c} C_C = 0 \qquad (2)$$

where $-\left(\frac{x}{c} C_N + \frac{z}{c} C_C\right)$ is the change in pitching-moment coefficient at a constant angle of attack caused by a change in center-of-gravity position.

[redacted]

Measured values of C_N and C_C were used for the various angles of attack. The values of C_C corresponded to those determined for configuration 2.

In order to enable the determination of C_{n_ψ} for a pitch trim angle corresponding to any center-of-gravity position, the curves of figure 6(b) were calculated with the use of the following relation:

$$C_{n_{\psi_1}} = C_{n_\psi} - \frac{x}{c} C_{Y_\psi} \tag{3}$$

Values of 0, -0.001, -0.002, and -0.003 were assumed for $C_{n_{\psi_1}}$ and experimental values of C_{n_ψ} and C_{Y_ψ} measured at several angles of attack were substituted in equation (3). The pilot-seat combination was assumed to be symmetrical in the spanwise direction and thereby assumed to trim always at 0° angle of yaw.

The curves of figure 6 indicate that large changes in static stability characteristics of the fin-stabilized seat would result from small displacements of the center-of-gravity position. As shown by figure 6(a), an upward displacement of the center of gravity of the order of 1.5 percent of the seat reference length would result in a decrease in the pitch trim angle from about 19° to about 3° and a decrease in the pitch stability. With the new pitch trim angle obtained from figure 6(a) it can be seen from figure 6(b) that the yaw stability would increase. A forward displacement of 1.5 percent would have a relatively smaller influence on the pitch trim angle but would increase the model pitch and yaw stability. Instability in yaw would result with any small rearward or downward center-of-gravity displacement.

Inasmuch as the solid curves of figure 6(a) were calculated with the use of the assumption that C_{m_α}, C_{N_α}, and C_{C_α} were constant throughout the angle-of-attack range and were equal to the average slopes measured between 10° and 20°, it would be expected that predicted pitching-moment slopes from figure 6(a) would be applicable only to this angle-of-attack range. In order to determine the limitations of figure 6(a), the pitching-moment curves for various center-of-gravity positions were computed point for point from the original experimental data and the pitching-moment slopes for several angles of attack between -25° and 25° were measured. These slopes are plotted in figure 7 and the values of the predicted slopes obtained from figure 6(a) are given for comparison; this comparison indicates that the pitch stability characteristics can be predicted accurately from figure 6(a) for angles of attack between approximately 2° and 21°.

[redacted]

Calculations of the effect of changes in center-of-gravity position on the static stability characteristics were also made for configuration 1 to determine the possibility of stabilizing the ejectable pilot-seat combination without the aid of stabilizing fins. These calculations indicated that the model can be made to trim at any angle of attack between 0° and 25° with stable pitching-moment characteristics. The model would remain unstable in yaw, however, unless the center of gravity is relocated at least 12 percent of the seat reference length forward of it present position. The magnitude of the center-of-gravity displacement required to obtain good static stability in yaw without fins is probably too large to be feasible.

Force Characteristics

The normal- and chord-force data obtained for the fins-off configuration through a Mach number range from 0.4 to 0.88 are presented as figures 8 and 9.

Normal- and chord-force characteristics.- An almost linear variation of normal-force coefficient with angle of attack resulted at each Mach number throughout most of the angle-of-attack range investigated. An increase in Mach number from 0.4 to 0.88 caused an increase in normal-force-curve slope from 0.016 to 0.022 at zero angle of attack. The magnitude of the chord force at any angle of attack is shown to increase with increasing Mach number. The rate at which these chord forces increase with Mach number becomes greater as the Mach number is increased.

Resultant forces.- Since the resultant force at the trim angle must pass through the center of gravity, the lines that denote the displacement of center of gravity required to obtain a given pitch trim angle (dashed lines in figure 6(a)) also denote the lines of action of the resultant forces on the seat of configuration 7 at a Mach number of 0.8. By superimposing the airstream direction for angles of attack between -10° and 25° on the coordinate system of figure 6(a), it will be seen that the direction of the resultant-force vector is never inclined with the air stream (drag) direction by an angle greater than 11°. This would indicate, therefore, that the principal force acting on the model is drag. The intersection of the resultant forces at a common point $\frac{x}{c} = -0.044$ and $\frac{z}{c} = 0.009$ for angles of attack between -10° and 20° locates the aerodynamic center of the model for this pitch range.

CONCLUSIONS

The results of an investigation made on a practical design model of an ejectable pilot-seat combination indicate the following general conclusions:

1. The instability of the pilot-seat combination was eliminated by the addition of stabilizing fins.

2. Large changes in the stability characteristics and trim angles resulted from variations in fin position, dihedral, or incidence angles and from small displacements of the center-of-gravity position.

3. The magnitude of the aerodynamic interference that exists about the seat had a large effect on the effectiveness of fins located at moderate distances from the seat.

Langley Aeronautical Laboratory
National Advisory Committee for Aeronautics
Langley Field, Va.

[redacted]

REFERENCES

1. Marzella, J., and Hess, J. R.: Ground and Flight Tests of Martin-Baker Aircraft Company Pilot's Ejection Seat from Model JD-1 Airplane. Rep. No. ASL NAM 256005.1, Part 1, Naval Air Experimental Station, Bur. Aero., Feb. 27, 1947.

2. Heinrich, Helmut G., and Berndt, Rudi: Stabilization of Pilot Ejection Seat. MR No. MCREXE-672-22H, Air Materiel Command, U.S. Air Force, July 16, 1948.

3. Viggiano, Louis R.: Test of a Full Scale Ejection Seat and Dummy with and without Stabilizing Flap Combinations Conducted in the Massie Memorial Wind Tunnel. Tech. Rep. No. 5778, Air Materiel Command, U.S. Air Force, Nov. 16, 1949.

1146.31
Lockheed/5

4. Santi, Gino P., Hill, Thomas C., Mazza, Vincent, and Carroll, Charles E.: Pilot Ejection Flight Tests Conducted with a TF-80C Airplane at Muroc and Hamilton Air Force Bases. MR No. MCREXA7-45341-4-1, Air Materiel Command, U.S. Air Force, Aug. 15, 1949.

5. Von Doenhoff, Albert E., and Abbott, Frank T., Jr.: The Langley Two-Dimensional Low-Turbulence Pressure Tunnel. NACA TN 1283, 1947.

6. Von Doenhoff, Albert E., and Braslow, Albert L.: Studies of the Use of Freon-12 As a Testing Medium in the Langley Low-Turbulence Pressure Tunnel. NACA RM L51I11, 1951.

[redacted]

Configuration	X'	Y'	Z'	Γ	i_f	a_f	b_f
①	No fins						
②	3.69	1.81	1.81	45°	-32°	1.06	1.38
③	3.69	3.75	1.81	-60°	-41°	1.94	1.38
④	3.18	3.26	1.42	-60°	-41°	1.94	1.38
⑤	3.18	2.54	1.42	-60°	-41°	1.94	1.38
⑥	3.18	3.26	1.42	-45°	-9°	1.94	1.38
⑦	3.18	3.26	1.42	-55°	13°	1.94	1.38

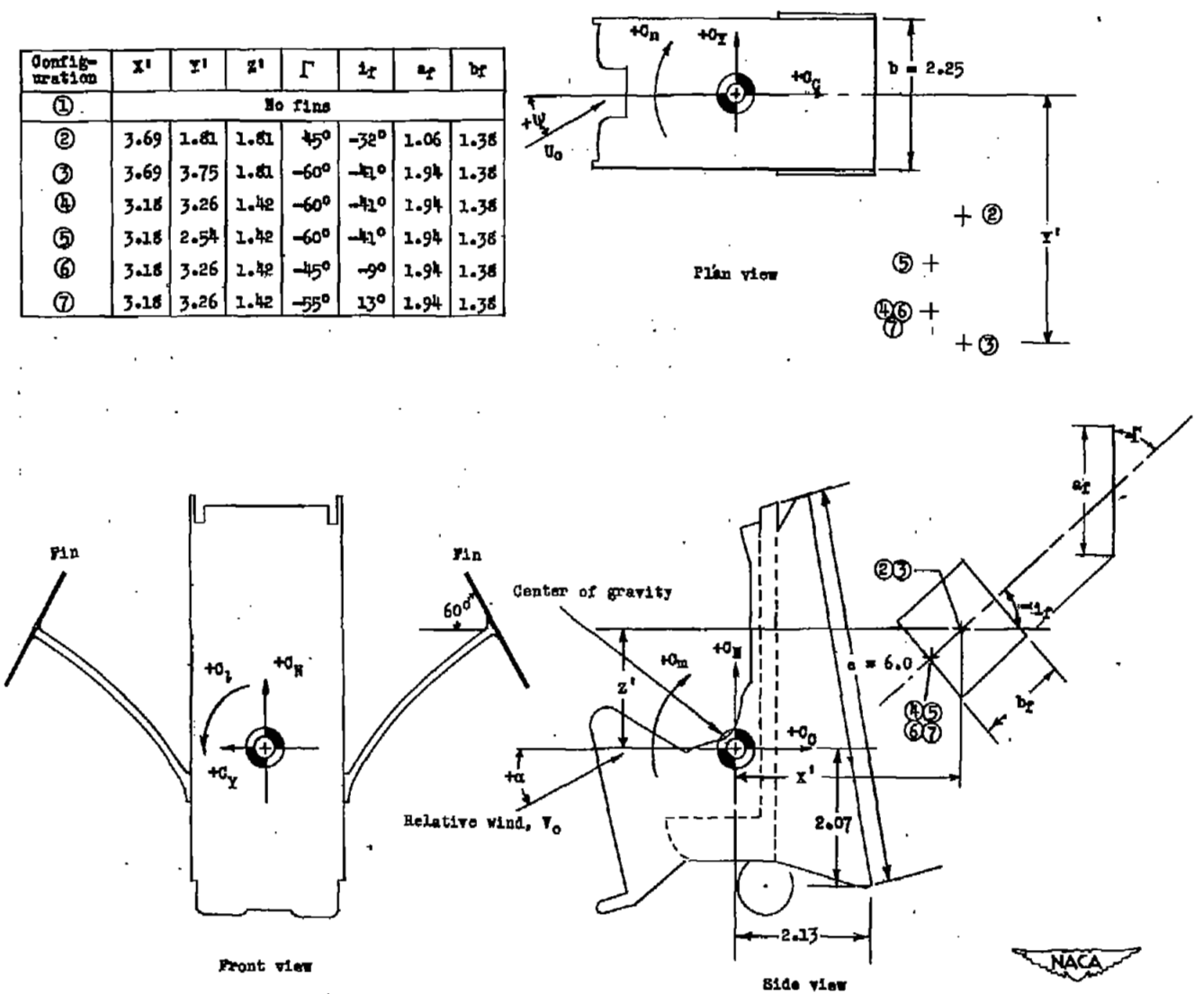

Figure 1.- Fin configurations investigated and definition of positive forces and moments on ejectable-pilot-seat model. All dimensions are in inches.

(a) Side view.

Figure 2.- Photographs of ejectable pilot-seat model. Configuration 7.

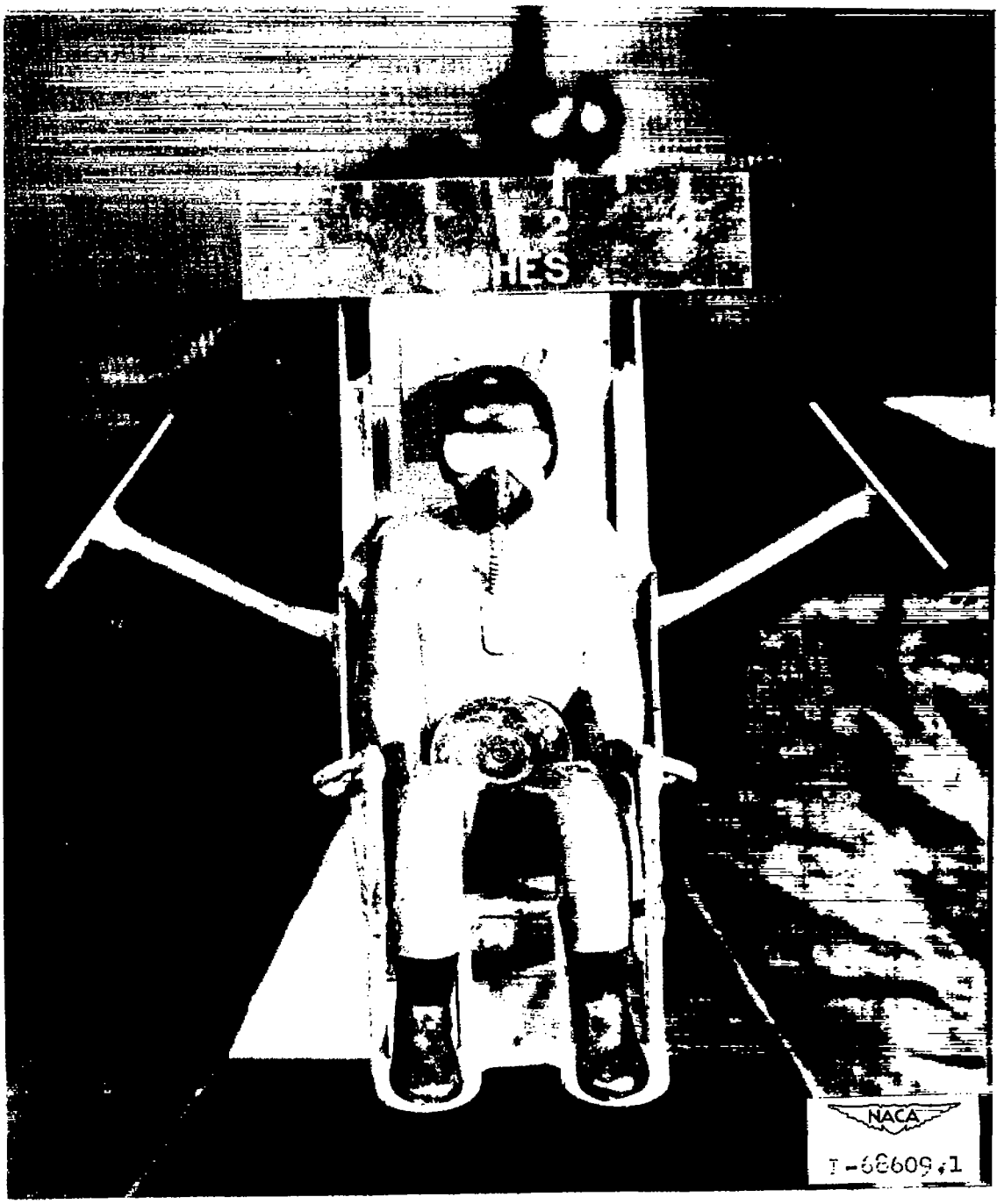

(b) Front view.

Figure 2.- Continued.

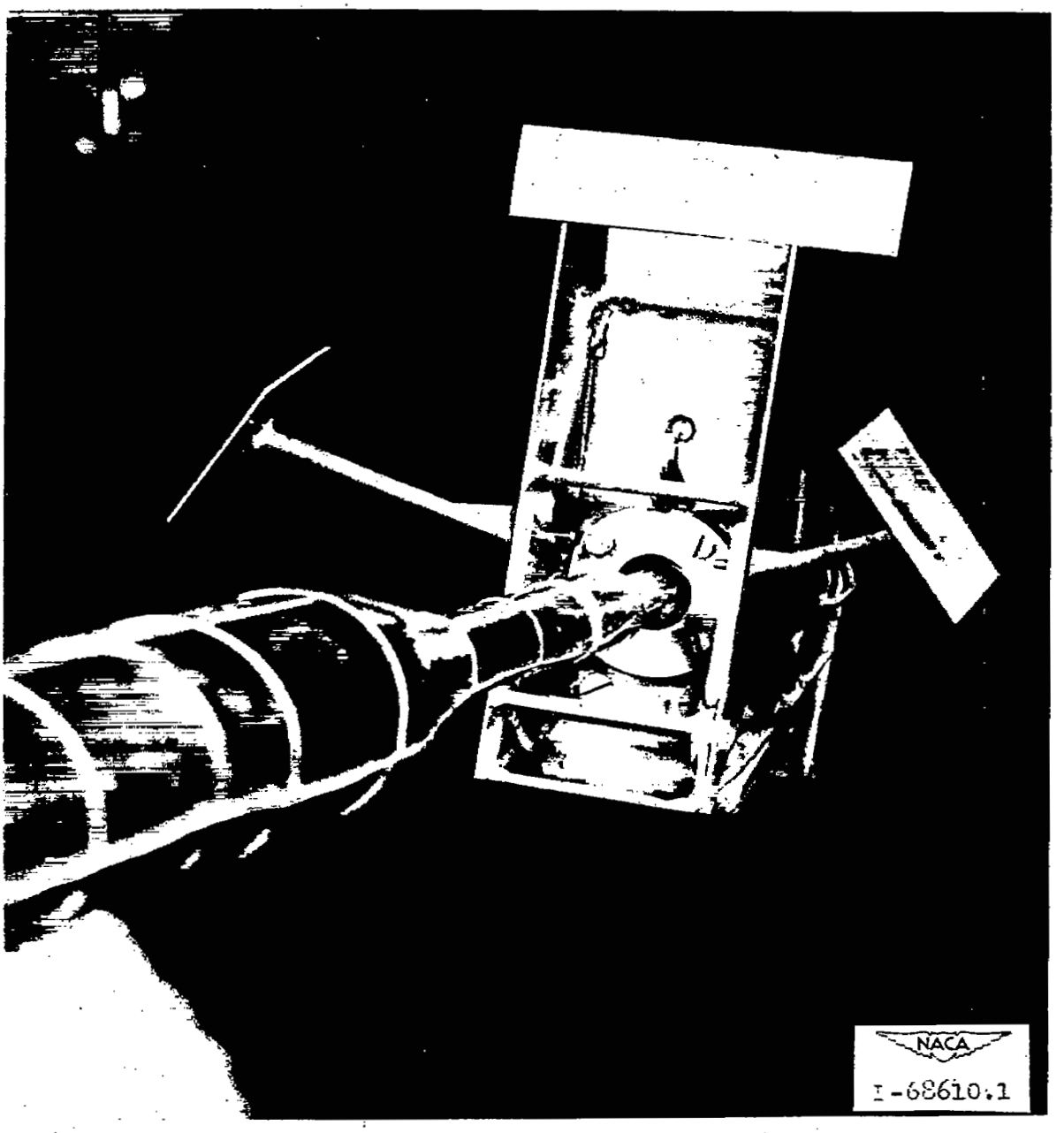

(c) Rear view.

Figure 2.- Concluded.

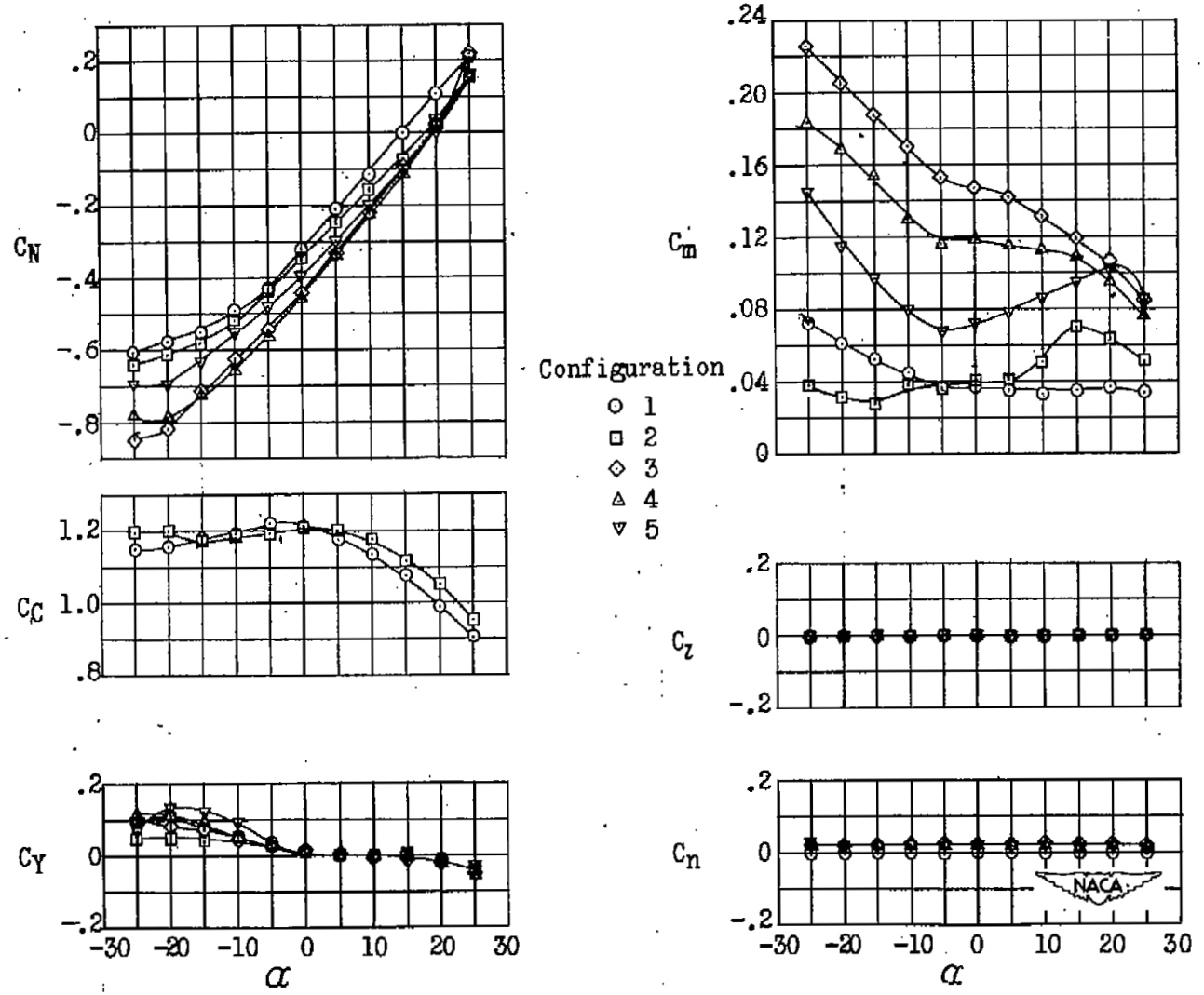

Figure 3.- Variation of aerodynamic forces and moments with angle of attack on model of ejectable pilot-seat combination. $\psi = 0^{o}$; M = 0.8.

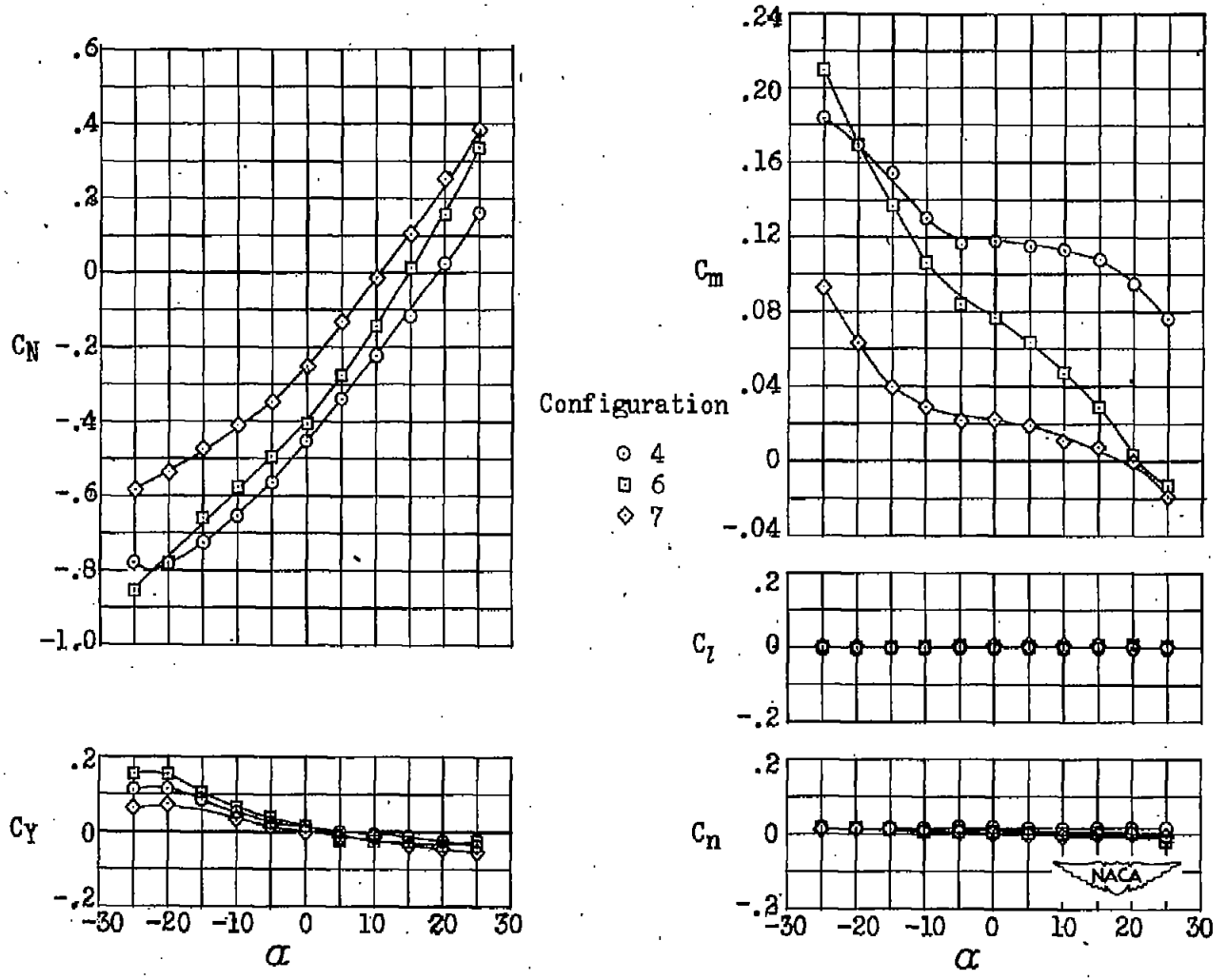

Figure 3.- Concluded.

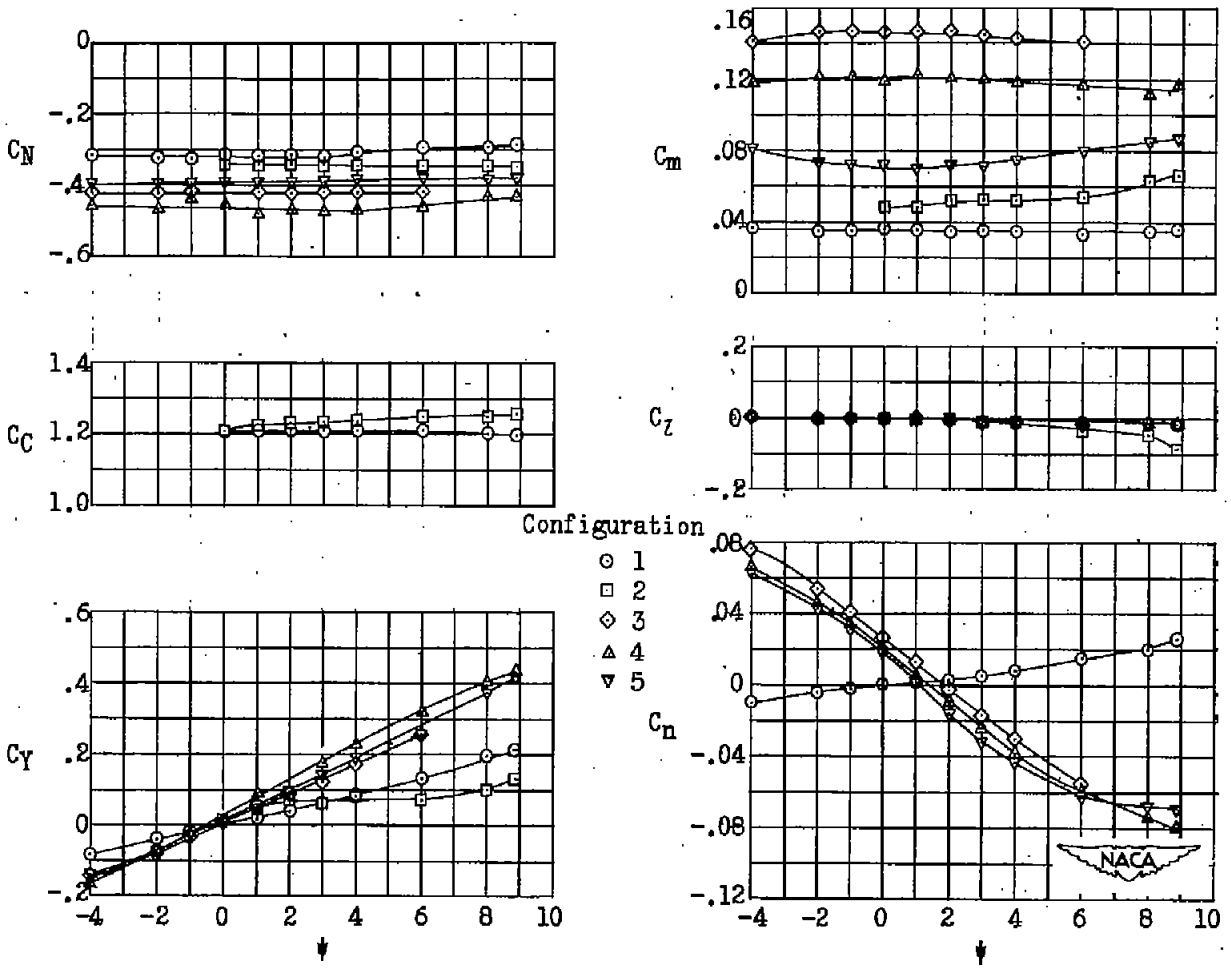

(a) $\alpha = 0^\circ$.

Figure 4.- Variation of aerodynamic forces and moments with angle of yaw on model of ejectable pilot-seat combination. M = 0.8.

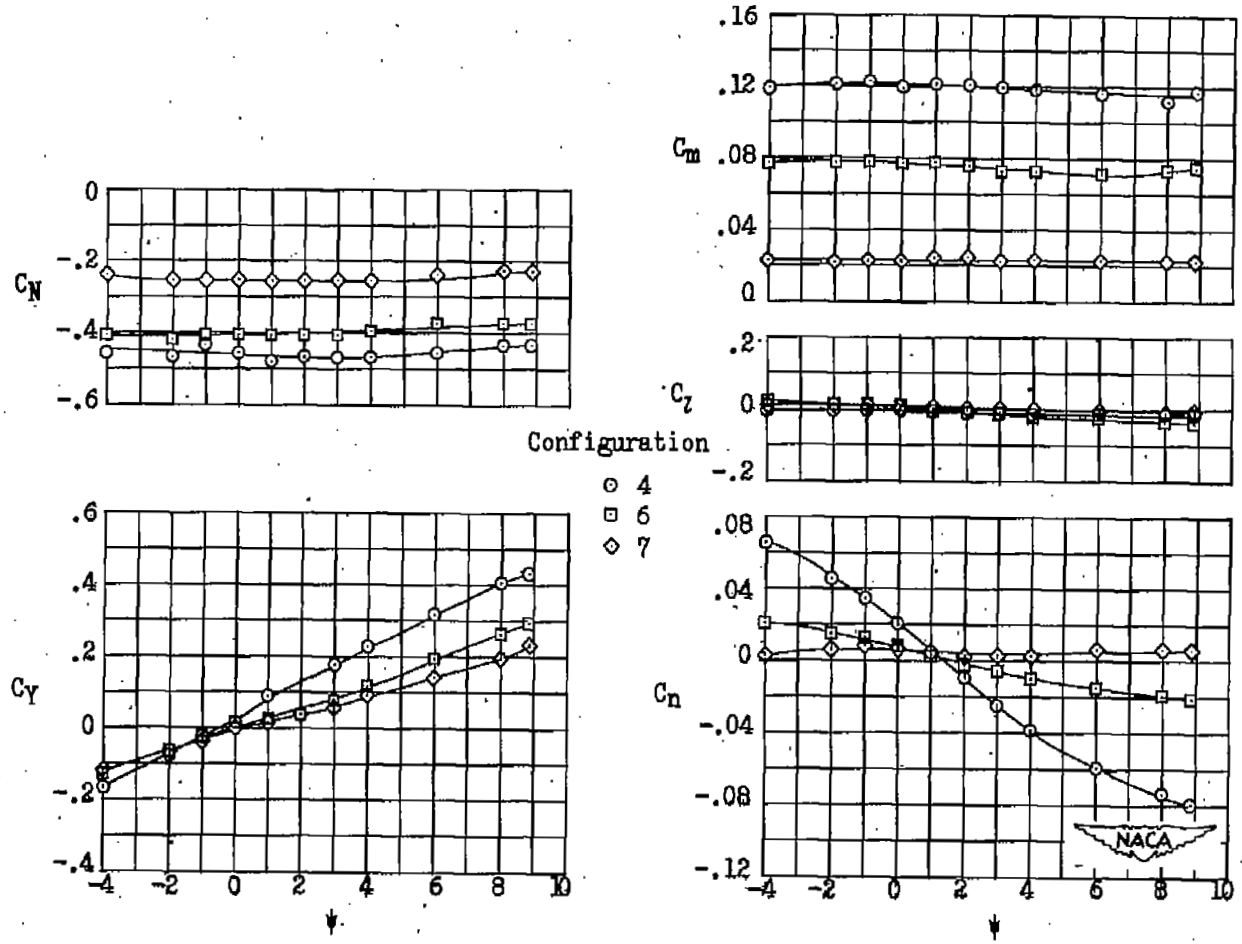

(a) Concluded.

Figure 4.- Continued.

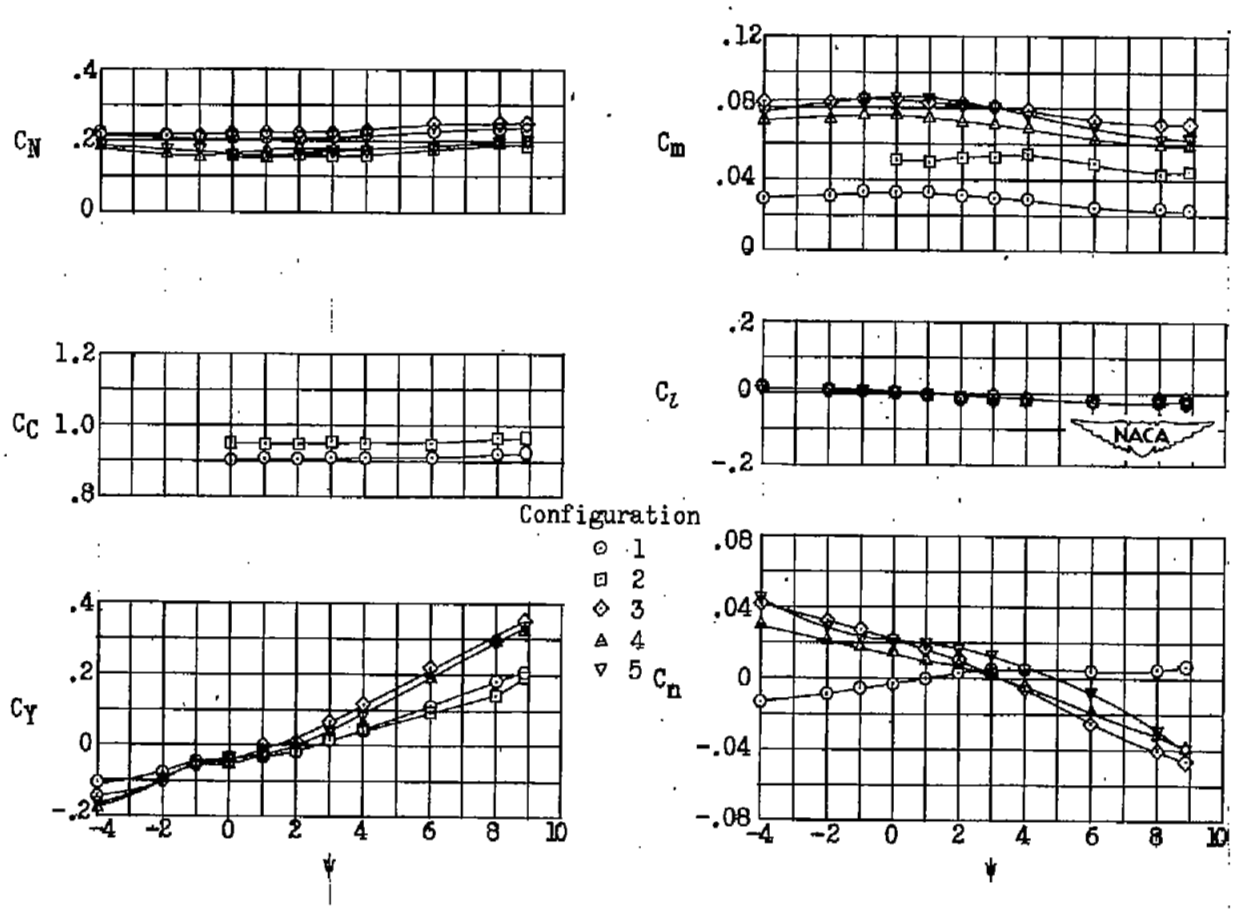

(b) $\alpha = 25°$.

Figure 4.- Continued.

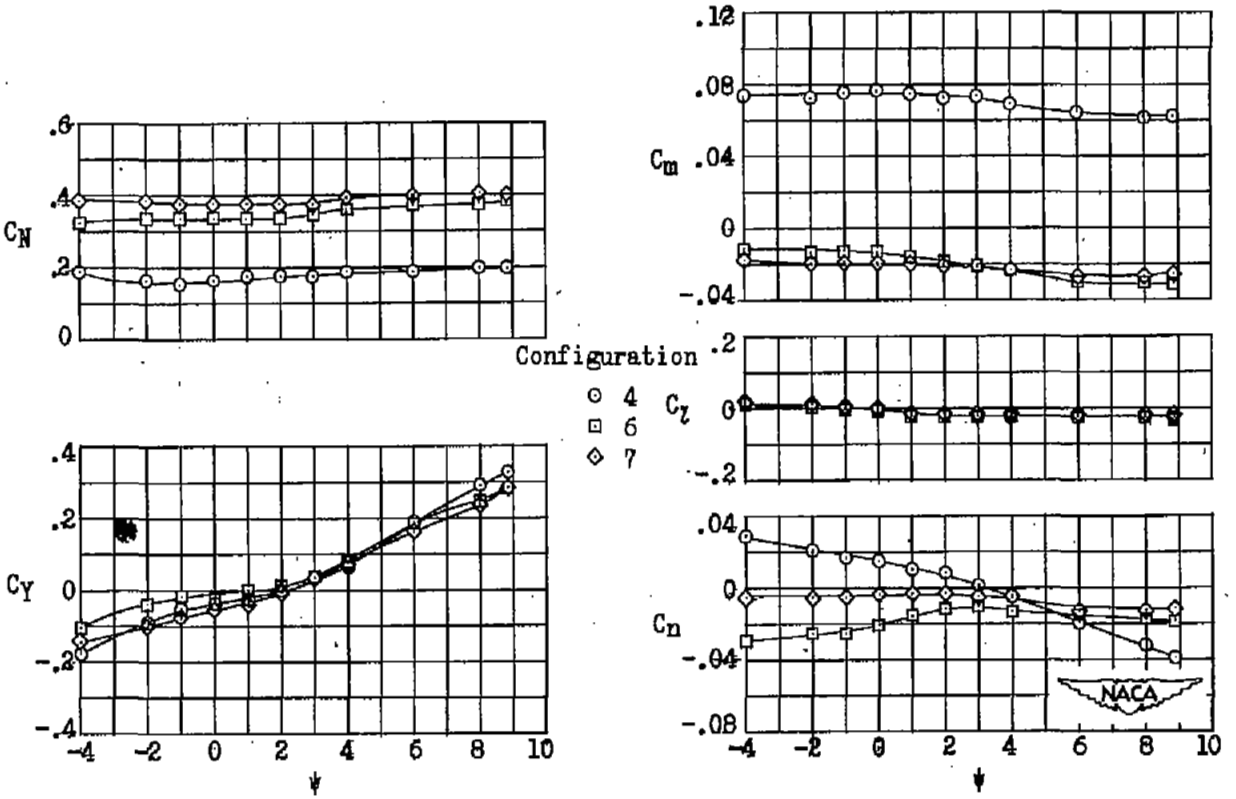

(b) Concluded.

Figure 4.- Continued.

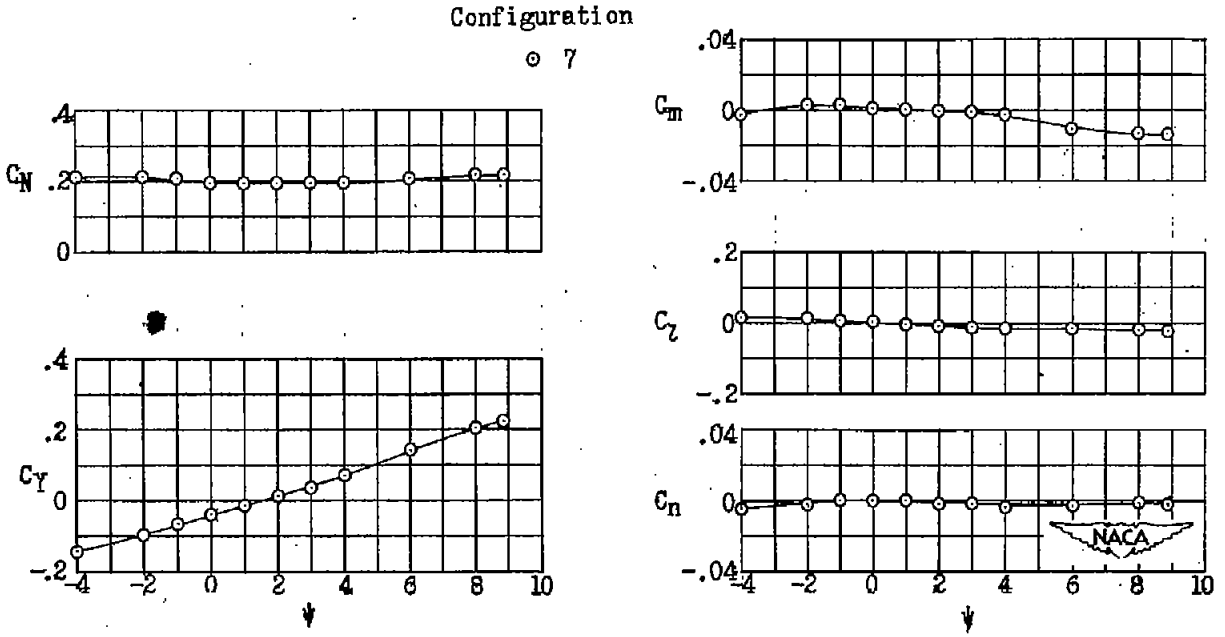

(c) $\alpha = 18.5°$.

Figure 4.- Continued.

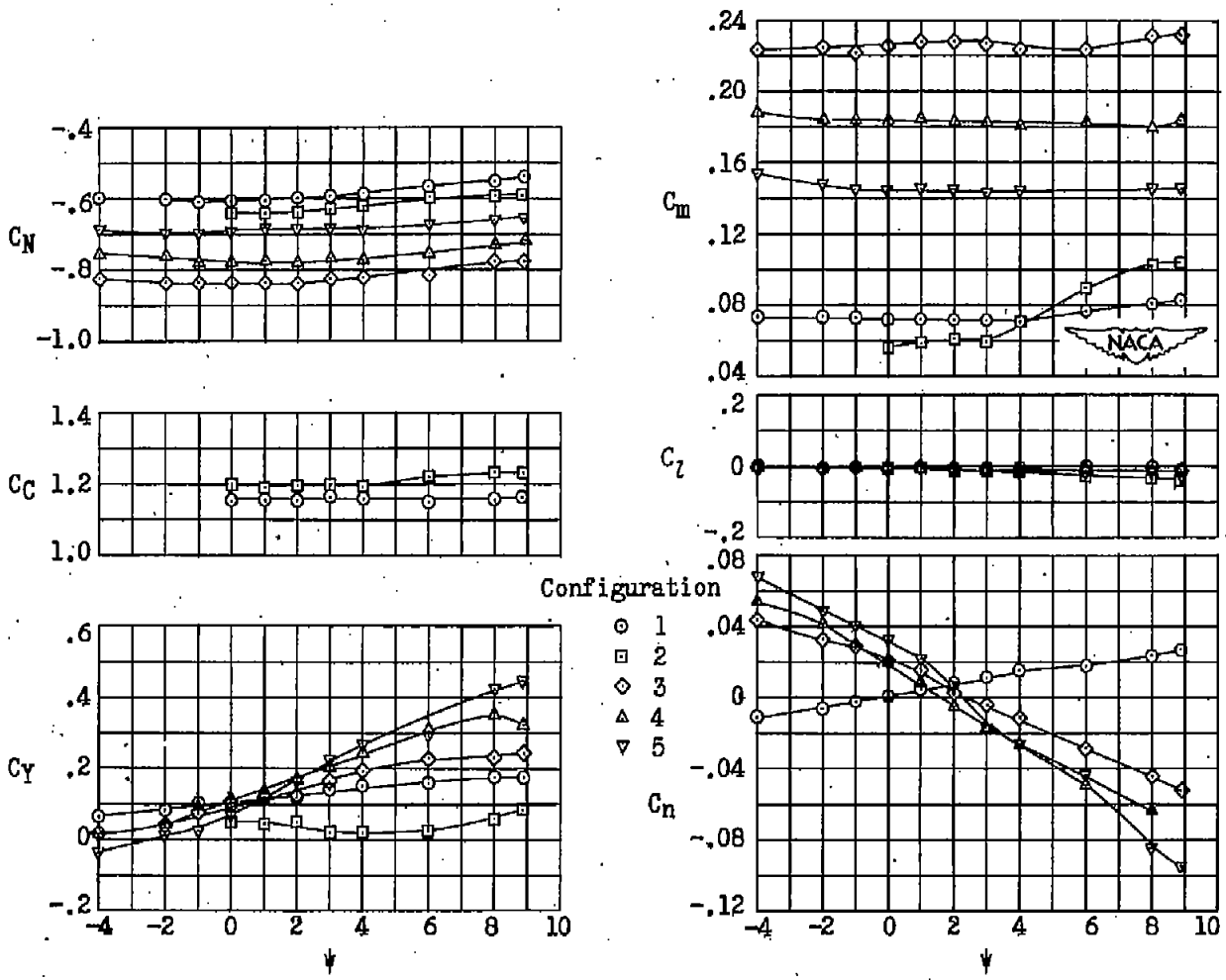

(d) $\alpha = -25^\circ$.

Figure 4.- Continued.

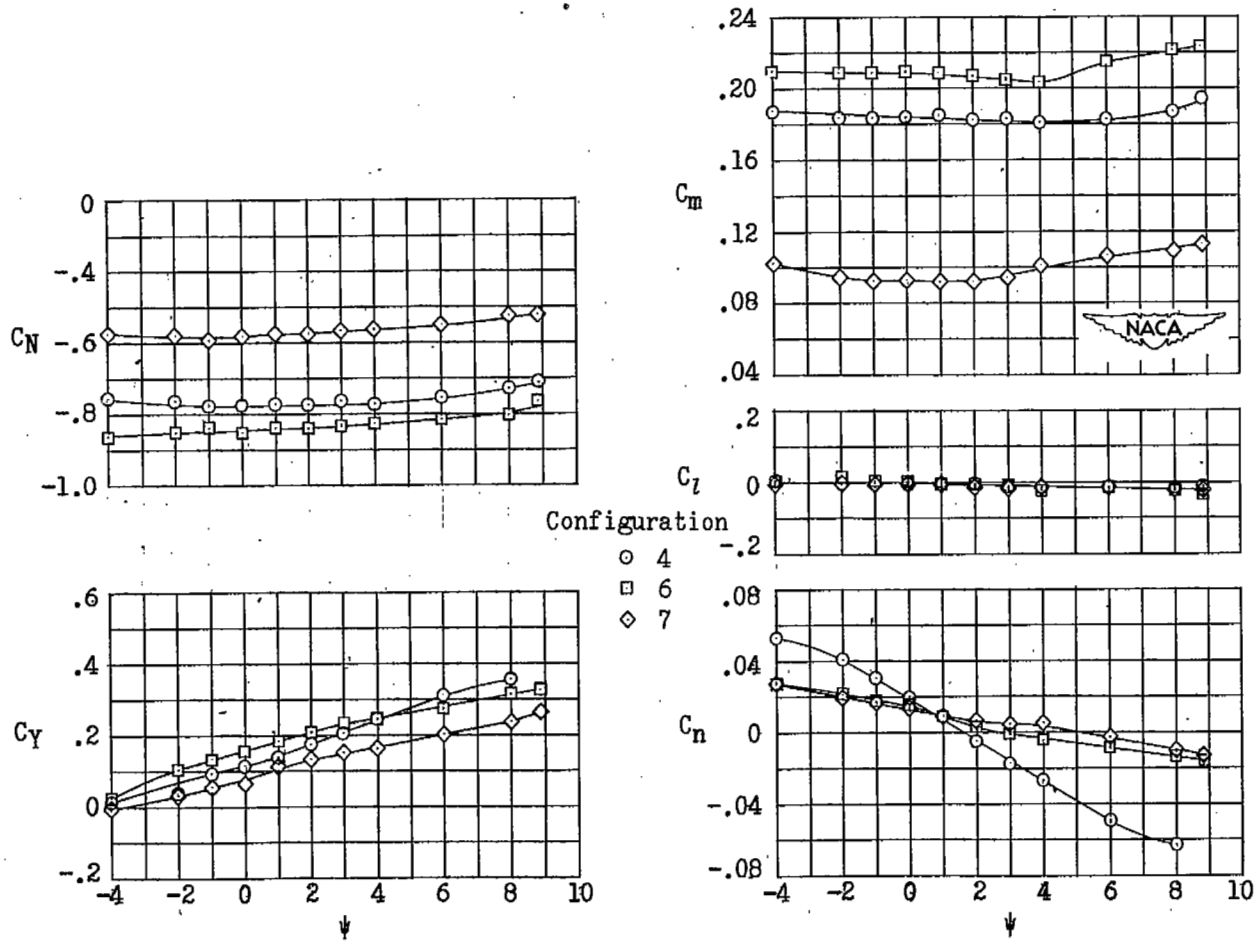

(d) Concluded.

Figure 4.- Concluded.

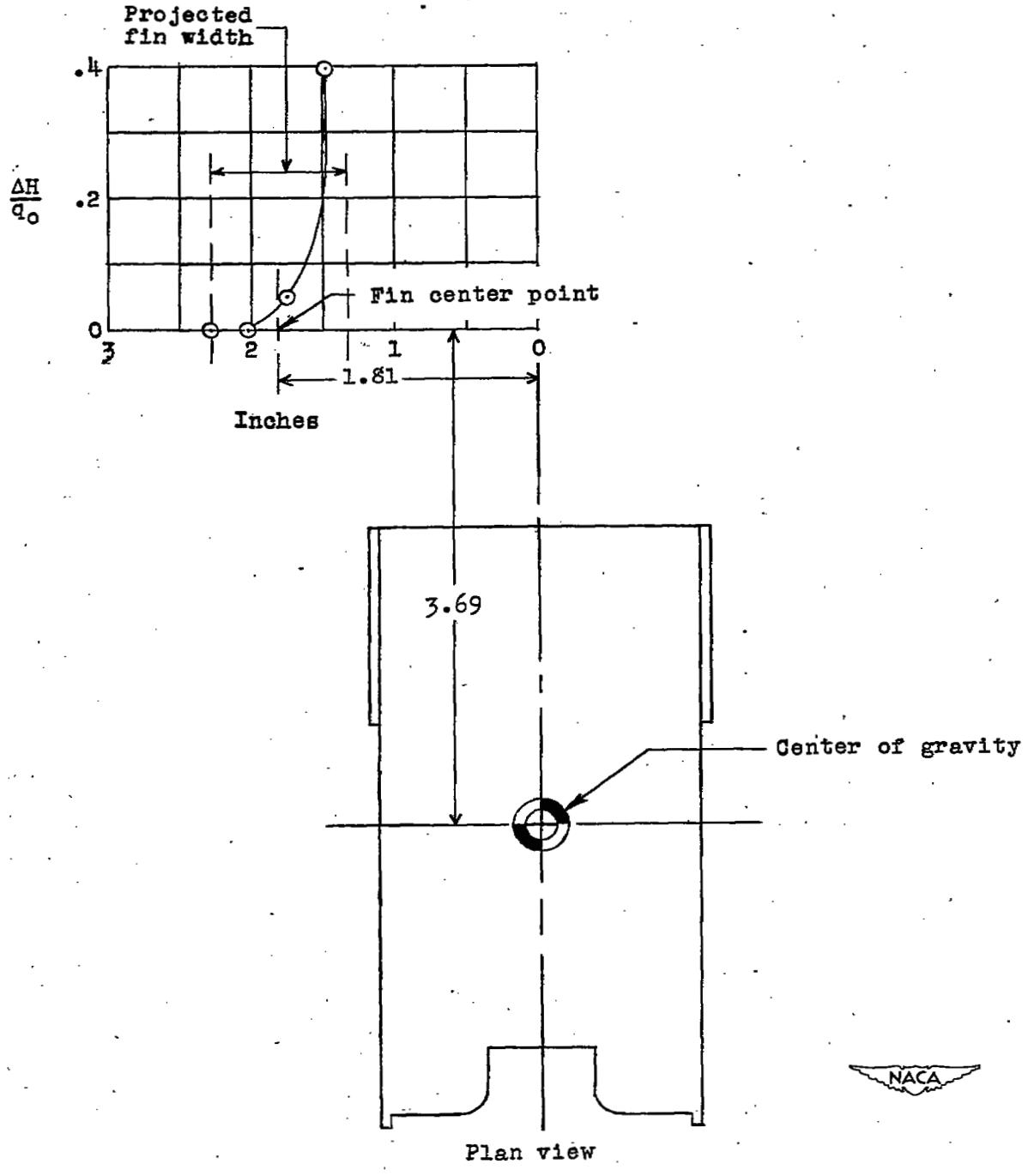

Figure 5.- Variation of total-pressure loss with spanwise distance at the vertical and longitudinal location of fins of configuration 2. M = 0.4; no fins.

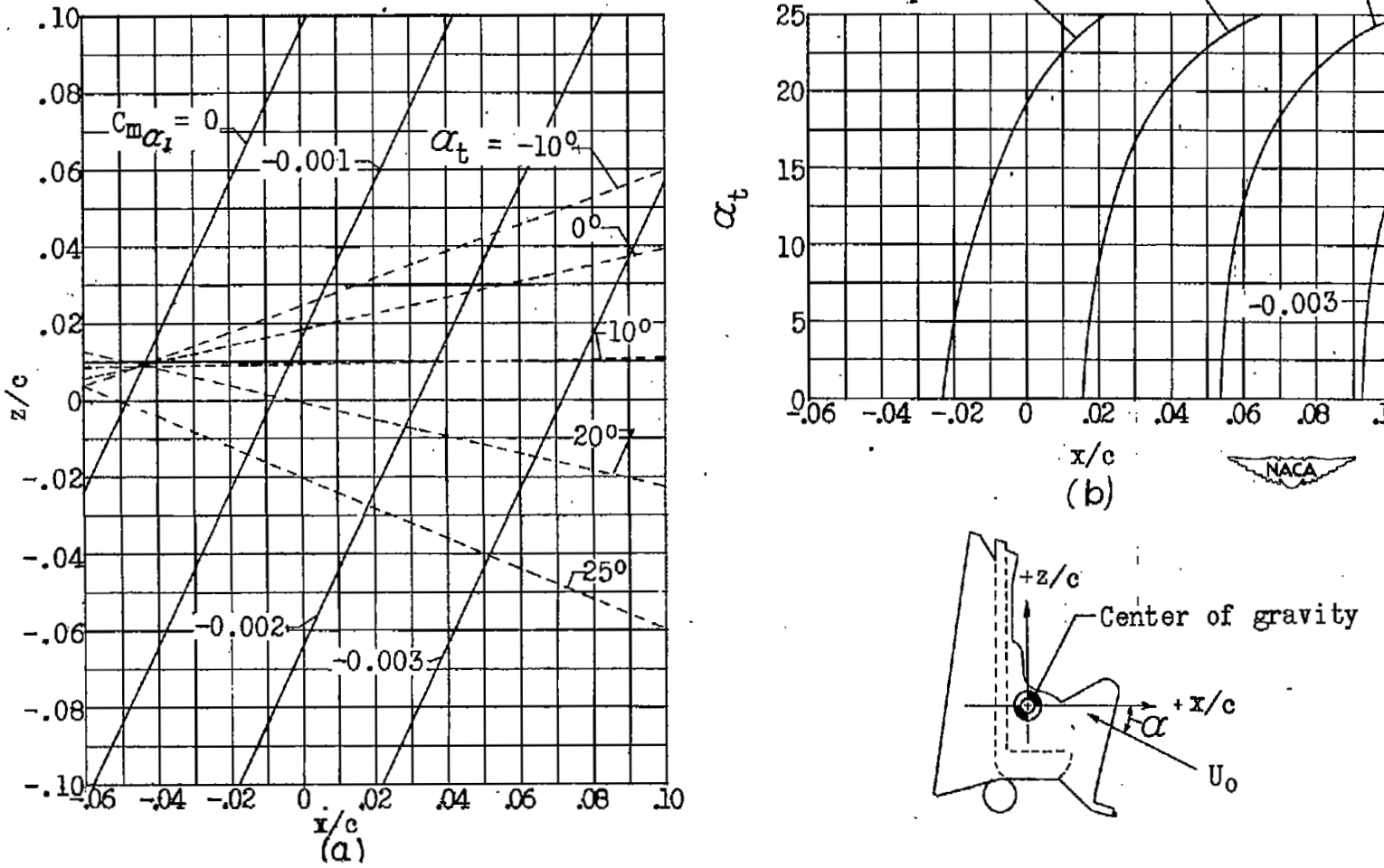

Figure 6.- Effect of center-of-gravity displacement on the stability characteristics of ejectable pilot-seat model. Configuration 7; M = 0.8.

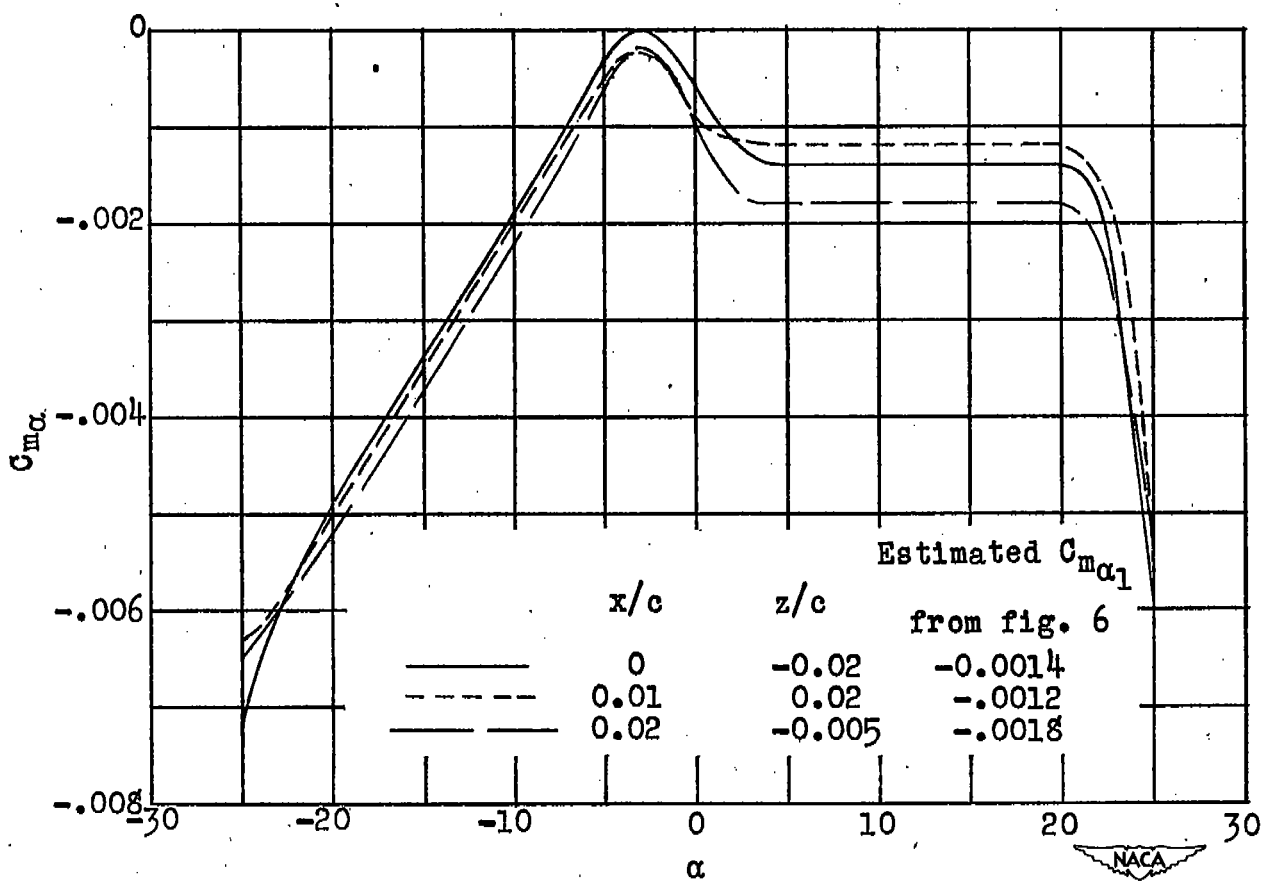

Figure 7.- Variation of C_{m_α} with angle of attack for three center-of-gravity positions of the ejectable pilot-seat model. Configuration 7; $\psi = 0^\circ$; M = 0.8.

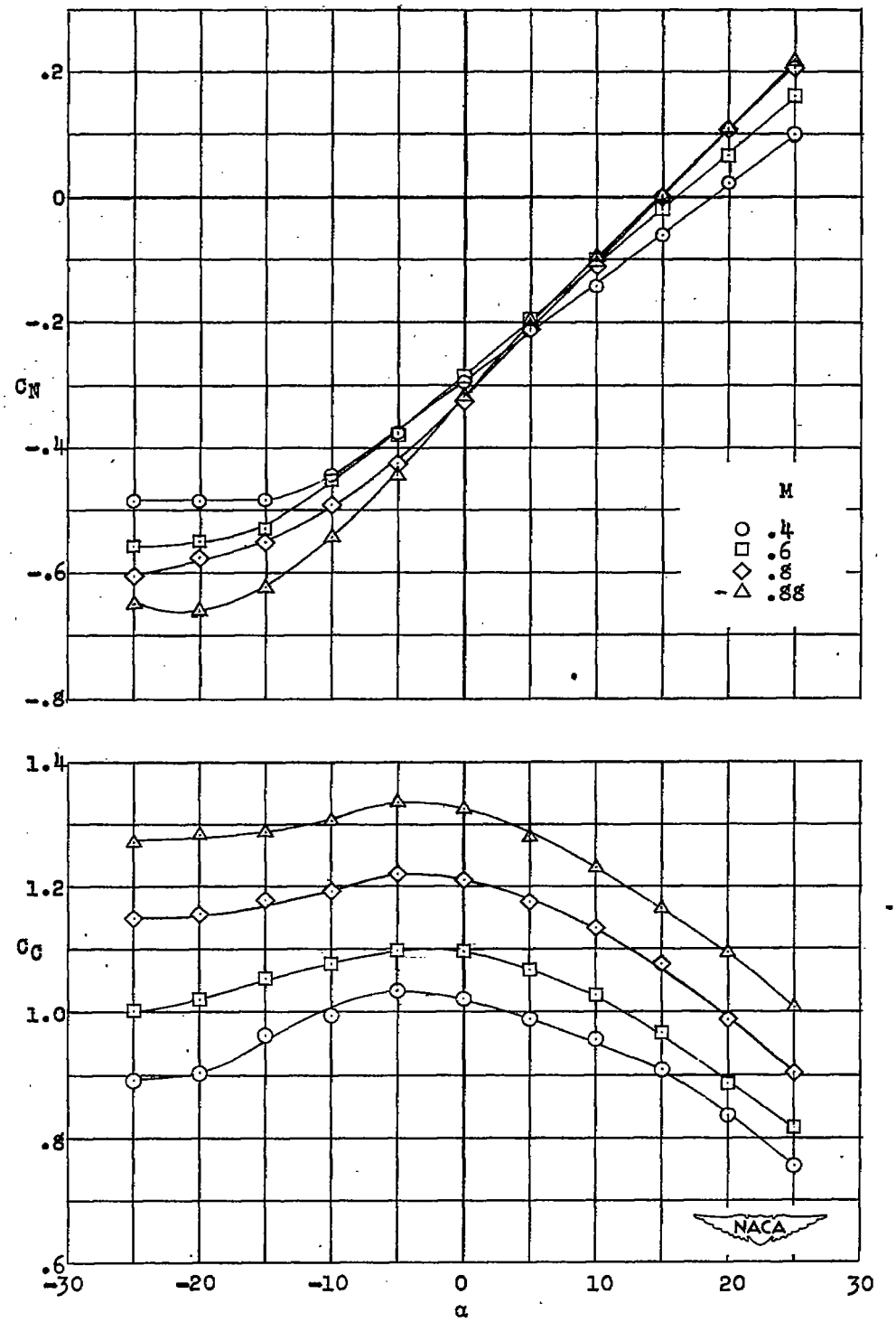

Figure 8.-Variation of normal-force and chord-force coefficients with angle of attack on ejectable pilot-seat combination. Fins off.

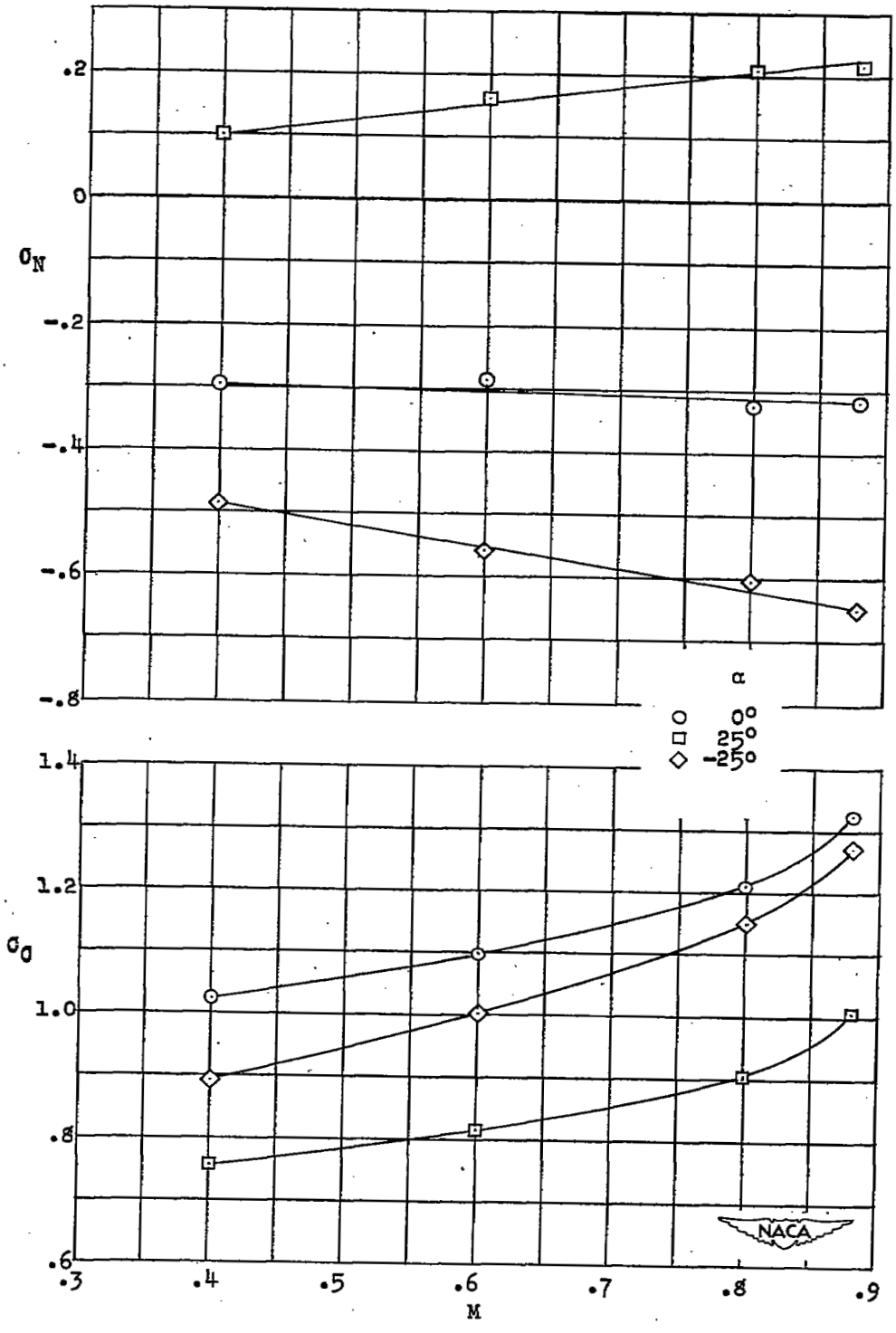

Figure 9.- Variation of normal-force and chord-force coefficients with Mach number on model of ejectable pilot-seat combination. Configuration 1.